Dynamics of railway wagons subjected to braking torques on defective tracks

Zuoyan Zhang[1] & Manicka Dhanasekar[2]

[1] Modeller, Parsons Brinckerhoff, Brisbane, QLD4001, Australia

[2] Professor, Queensland University of Technology, Brisbane, QLD4000, Australia; m.dhanasekar@qut.edu.au

Post Review Final Version to:

International Journal of Vehicle System Dynamics

Jan 2011

Abstract

It is well known that track defects cause profound effects to the dynamics of railway wagons; normally such problems are examined for cases of wagons running at a constant speed. Brake/traction torques affect the speed profile due to the wheel-rail contact characteristics but most of the wagon-track interaction models do not explicitly consider them in simulation. The authors have recently published a model for the dynamics of wagons subject to braking / traction torques on perfect track by explicitly considering the pitch degree of freedom for wheelsets . The model is extended for cases of lateral and vertical track geometry defects and worn railhead and wheel profiles. This paper presents results of the analyses carried out using the extended model to the dynamics of wagons containing less than ideal wheel profiles running on tracks with geometry defects and worn rails.

Keywords: braking/traction torque, wheel unloading, track irregularity, wagon yaw, wagon roll, worn rail/wheel

1. Introduction

Wagon operations are commonly associated with braking/traction especially when they enter and exit speed restriction zones and/or tight curves. Most of the wagon dynamics simulation packages that primarily focus on long distance route simulations routinely require pre-defined

speed profiles for dealing with those situations. Such simulation algorithms usually do not include wheelset pitch and hence cannot be explicitly used for the modelling of the wheelset slip and skid expected under severe braking torques.

This paper refers to a mathematical formulation of full wagon systems acted upon by traction/ braking torques using a fixed coordinate reference system both in space and time published by the authors recently [1]. With this formulation the complex behaviour of the wagon dynamics under braking/traction torques can be truly modelled without any need for working out the speed profile as *a priori*. Our previous paper focuses on wagons that run on perfect track under the influence of normal and severe levels of traction and brake force sequences; Wheelset skidding, wheel unloading and wagon pitch are also reported [1].

The current paper has extended our previous model to cases of track irregularity and worn rail/ wheel profiles. Effects of the lateral track irregularities to the yaw moment and different vertical sinusoid and plateau defects to the wagon roll are reported in this paper. The track defect effect on wagon pitch and worn rail/wheel profile study are also presented.

2. Literature Review

Rotational motion of wagons includes pitch, yaw and roll, which are sparingly reported in the literature. The paucity perhaps is linked to the steady state focus of most system simulation packages. The effect of bogie and wagon pitch induced by the longitudinal forces was examined experimentally through an instrumented bogie by McClanachan et al. [2]. The prevalence of light duty vehicles has prompted investigations into methods to reduce the vehicle body roll by Climb et al. [3].

The study of imperfect rails is mainly used to address ride characteristics and ride comfort. Comprehensive rail geometry definition and properties can be found in Dukkipati [4]. The geometry of wheel/rail profiles affects the creepage/creep and adhesion and they in turn result in the complex dynamic behaviour of wagons. Vibration characteristics of track are the result of cumulative forces and the source of increased stress, energy losses, additional wheel/rail wear and passenger discomfort. Therefore, study of these characteristics and influences of the rail profile can offer excellent source of information for the maintenance purpose. However, the irregular rail profile concerned with corrugation which falls into the non-steady category

and the wheel/rail discontinuities such as the insulated rail joints, turnouts and switches are not discussed here.

By introducing surface parameters [5], Pombo et al. [6] proposed a general geometric track description which integrates track irregularities as a function of the track length to the dynamics of the wheel/rail contact simulation. A simulation of the influences of periodic track irregularities on a freight car was carried out by Chen and Jin [7]. Li et al. [8] developed a real time technology to predict vehicle performance based on the track geometry. Steenbergen [9, 10] investigated the relationship between different stages of wheel flats and wheel/rail interaction.

Detailed description on wagon brake system is provided in [1]. Air brake system responses rely on the air transmission speed of the brake pipe drop rate. Parametric study of railway air brake system was given by Murtaza and Garg [11] and Piechowiak [12]. Cocci et al. [13] developed a multibody system (MBS) model to perform braking simulation and compared it with the experimental tests. Chou and Xia [14] proposed a controlled pneumatic brake system to minimise the running costs of heavy-haul trains. Olson [15] developed single- and two-wheel braking models to investigate ground vehicles. Malvezzi et al. [16] built a new speed control system to analyse braking performance. The braking performance was assessed through a function of several general parameters. Durali and Shadmehri [17] reported an analysis of train derailment due to severe braking. The most comprehensive review that summaries 80 years on brake vibration and/or noise was given by Cantoni et al. [18].

Handoko and Dhanasekar [19,20] reported a fixed reference frame formulation of a bogie model. Lateral and vertical track irregularities were input to the bogie-track system to generate vibration for studying bogie yaw and roll moments plus lateral and vertical displacements of wheelsets. A sequence of longitudinal torque was applied to railway bogies to investigate the bogie pitch moment. Bogie dynamics under heavy braking was presented in Handoko [21], which also examined the effect of unevenly distributed brake torques applied to wheelsets.

3. Wagon model description and formulation

A wagon consisting of one wagon body supported by two bogies one at the front and the second at the rear, with each fitted with two wheelsets each and connected by mass less elastic springs and dampers as presented in [1] is considered in this paper. This model employs the fixed coordinate system introduced in [5]. Therefore contact kinematics are calculated as a function of the variation of the velocity of the moving body and calculated in real-time during the simulation process. Also, the effects of the severe application of heavy braking and traction such as skid and slip can be accounted for in this formulation. Details of the coordinates, formulations of wagon model, parameters used in wagon model can be found in [1] and hence are not reproduced here.

3.1 Extended formulation for defective tracks

Track irregularities are rectified with due care during track maintenance because excessive wagon response can result due to track disturbances leading to poor ride quality. With track imperfections combined with large brake and traction torques applied on wheelsets, the situation can even be more dangerous, but not well understood.

In this study, sinusoidal lateral track irregularities are found to affect the yaw moment and other specific features of wagon movement through changes to the vehicle speed, which in turn is affected by the defect amplitude and applied brake torques. Different vertical sinusoid and plateau defects are used to exploit the wagon roll and pitch. The influences of brake and traction torques on wheel unloading and wagon yaw and wagon roll are illustrated through numerical examples.

3.1.1 Lateral irregularity of track

A general sinusoidal rail alignment irregularity may be expressed as in Equation (1).

$$Y(x) = \Delta_{ir} \sin(\pi k_{ir} x) \qquad \text{Equation (1)}$$

where Δ_{ir} is the amplitude of the defect and *k* is a parameter that defines the sine wavelength. In the simulation, Δ_{ir} is chosen from 5mm to 25 mm while k_{ir} is set as $0.045\,m^{-1}$ that corresponds to a wavelength of 44.44m. The irregularity was assumed to occur at the 25^{th} m of the track with the view to ensuring suppression of the effect of initial condition on wagon response.

3.1.2 Vertical irregularities of track

Track was assumed to exhibit sinusoid defects at the same location of both rails as defined below:

$$Z(x) = \Delta_{ir} \sin(\pi k_{ir} x) \qquad \text{Equation (2)}$$

The sinusoid defect was then assumed to occur on the left and right rails with a phase angle difference of 180° and 90° respectively. The analytical representation of these sinusoidal irregularities is expressed in Equations (3) and (4):

$$Z_L(x) = \Delta_{ir} \sin(\pi k_{ir} x + \pi/2) \qquad \text{Equation (3)}$$

$$Z_R(x) = \Delta_{ir} \sin(\pi k_{ir} x + \pi/4) \qquad \text{Equation (4)}$$

In the Equations(2)(4), *x* is the longitudinal travel and *Z* is the vertical height of the rail. Suffix *L* and *R* stands for left and right rail respectively. The cross level due to the sinusoidal phase difference is provided in Equation (5):

$$Z_C(x) = \left| Z_L(x) - Z_R(x) \right| \qquad \text{Equation (5)}$$

A plateau type defect (cross level) was assumed to occur only on the right rail in the examples whilst the left rail was kept perfect. The defect is mathematically expressed as:

$$Z_C(x) = \sqrt{\Delta_{ir}{}^2 / (1 + (k_{ir} x)^8)} \qquad \text{Equation (6)}$$

where Δ_{ir} is the amplitude and k_{ir} is a parameter that defines the sine wavelength.

Analyses carried out using the track shape containing sinusoidal vertical defect (Equation(2)) is termed as studies "case# S1" for convenience. Similarly, the two vertical defect situations with phase difference (Equations (3) and (4)) are termed as "case#S2" and "case#S3" respectively. The plateau case is termed as "case#C" in this paper.

4. Effects of Track Defect on Wagon Yaw

4.1 Speed influence

The wagon was considered to run over the sinusoid lateral defect with the amplitude of 10mm as shown in Figure 1. All case studies use the same shape shown in this figure which extends across the distance of 44.44m precisely but with differing amplitudes. The influence of speed (viz, 15m/s and 25m/s) to the wagon dynamics was examined through the yaw motions of the wagon body exhibited in Figure 2 that shows the magnitude of wagon body yaw increased with the operating speed; 50% larger yaw moment for 25m/s case was located at the 53rd m of the track. After the wagon transited the lateral defect, the wagon body yaw damped in the natural manner for 15m/s and 25m/s cases, albeit it took longer time to stabilise Under the influence of larger speed.

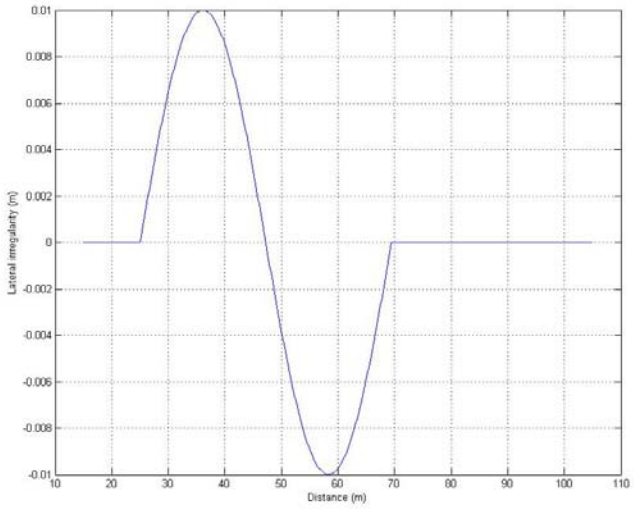

Figure 1. Input lateral track irregularity, different amplitude, same location

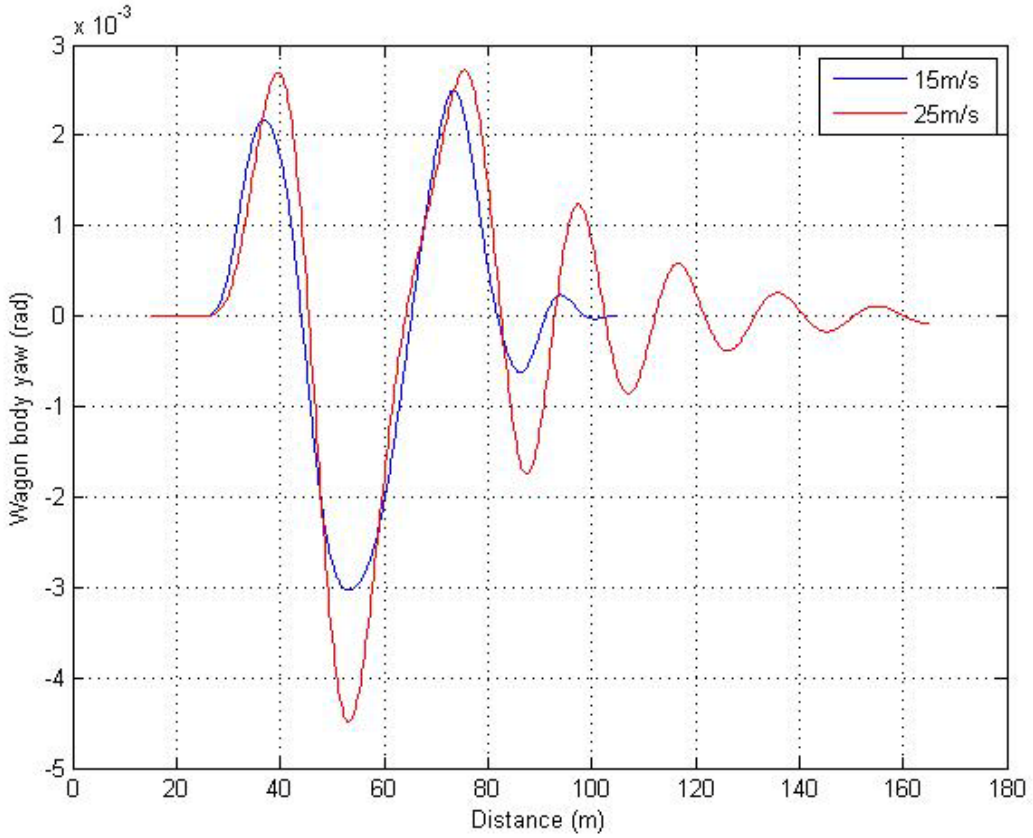

Figure 2. Wagon body yaw motion for 15m/s and 25m/s cases

4.2 Defect magnitude influence

This section reports the results of wagons running over the sinusoid lateral defects with an initial speed of 25m/s (this speed decreases slightly at the end of simulation due to energy loss). Five amplitudes of the defects (5mm, 10mm,15mm, 20mm and 25mm) were considered. The lateral displacements of wheelsets and the front/rear bogies and wagon body yaw responses are presented in this section.

Figure 3 shows the front bogie yaw and rear bogie yaw moment for 5mm to 25mm defects. All cases have exhibited two positive peaks and one negative peak, and the second positive peak value has been found to be larger and the negative peaks always have given the absolute maximum value. The magnitude of yaw moment is also generally proportional to the magnitude of the track defect. It is worthy of mention that the negative peaks among 5mm to

20mm are relatively smooth, whereas a fluctuation was found in 25mm because flange contact has occurred. Figure 4 describe the wheelset' lateral displacements for the 25mm defect case (Wheelset 1 refers to the front wheelset in front bogie and Wheelset 4 refers to the rear wheelset of the rear bogie with the other two in sequential order); it can be seen that flange contact lasts for about 10m travel of each wheelset.

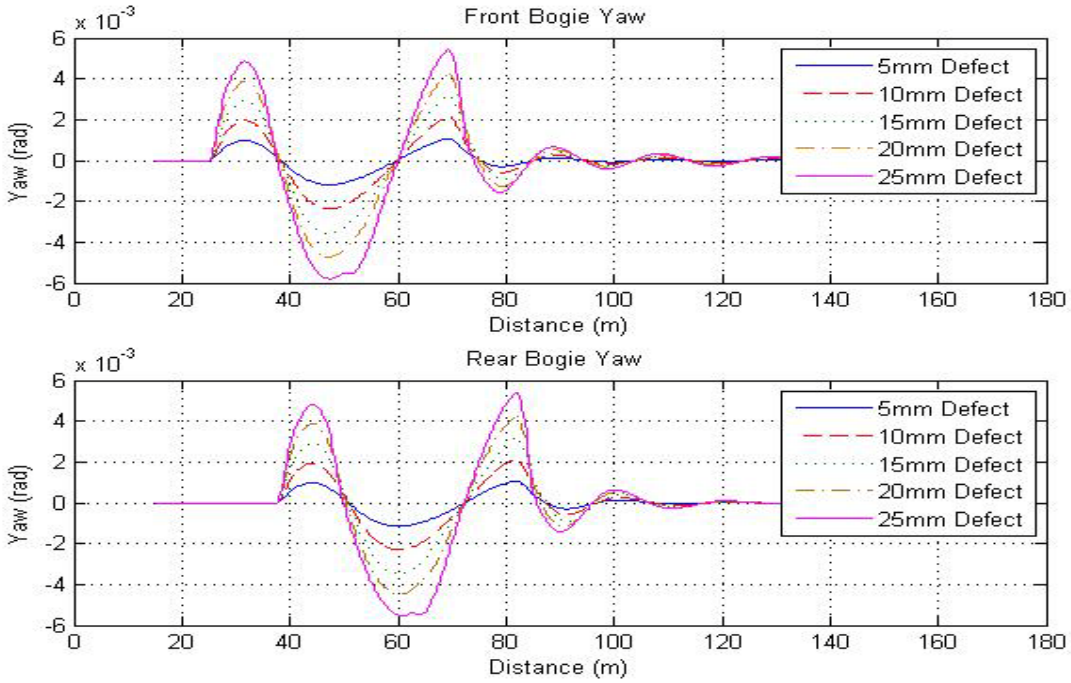

Figure 3. Front and rear bogie yaw motion for 5mm – 25mm defect cases

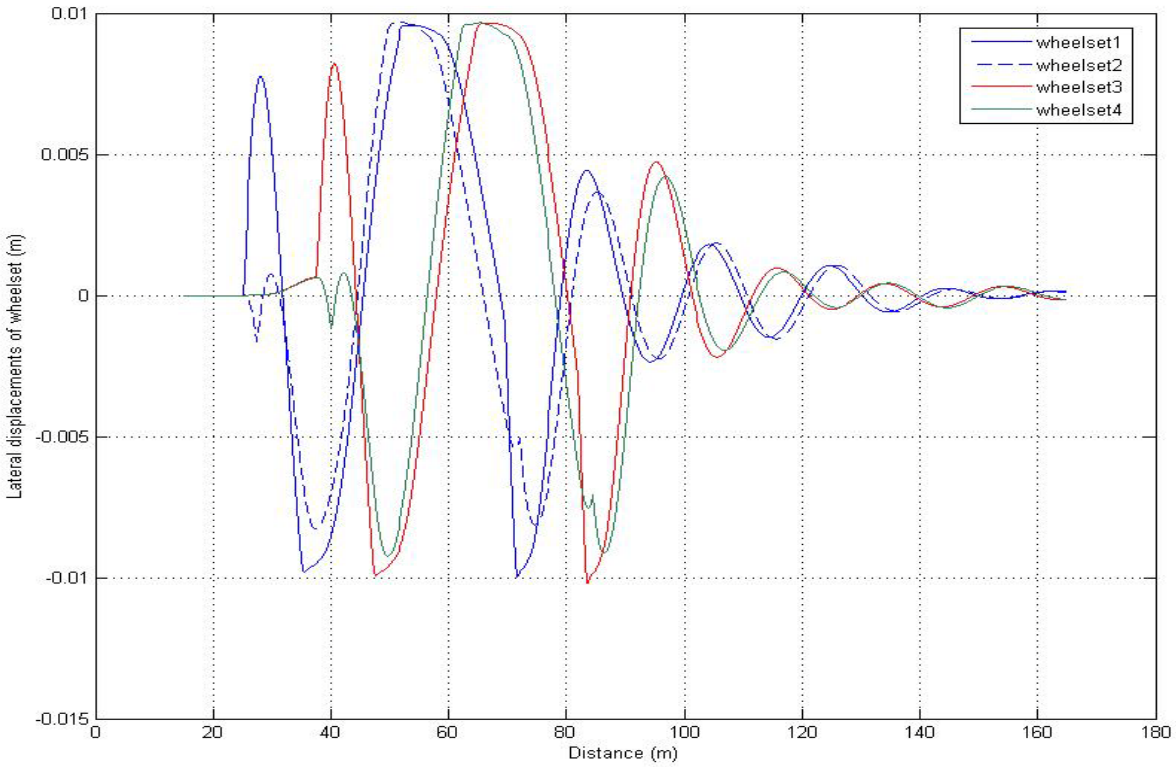

Figure 4. Lateral displacements of wheelsets (25mm defect case)

Table 1 illustrates the relationship of lateral track irregularity and negative bogie/wagon body yaw and their corresponding track distance. It implies that the track shape plays a predominate role on yaw moment response. The magnitude of yaw is generally proportional to the magnitude of the track defect, but the relationship is not strictly linear; the corresponding track distances, which means where the largest yaw occur, are relatively consistent. From Figure 1 we can see that the 47th m corresponds to the track defect balance position while the 60th m shows the negative peak. The maximum wagon body yaw has occurred between the negative peaks of the front bogie and rear bogie, and its value is approximately double that of the bogie's negative peaks.

Table 1. Magnitude and location of maximum negative yaw under lateral irregularity

Track Defect	Front bogie (10^{-3} rad)	Dist (m)	Rear bogie (10^{-3} rad)	Dist (m)	Wagon body (10^{-3} rad)	Dist (m)
5mm	-1.2	47.3	-1.1	60.0	-2.2	53.3
10mm	-2.4	47.3	-2.3	60.3	-4.5	53.3
15mm	-3.6	47.0	-3.5	60.0	-6.7	53.3
20mm	-4.7	47.0	-4.5	60.5	-8.7	53.0
25mm	-5.8	47.5	-5.5	60.7	-10.5	53.0

** these results are drawn from the 25m/s case study as set out in section 4.1.

4.3 Lateral dynamics under brake torque

The wagon was considered travelling on a track with sinusoidal rail alignment irregularity of 10mm amplitude as shown in Figure 1, whilst wo sorts of brake torques, 3.5kNm and 10kNm, were applied equally to each wheelset and for the distance from the 25th m to the 95th m. Noting that wheelset 4 leaves the track defect on the 85th m, an additional brake torque was applied for 10m travel to examine the trend of braking on perfect rail. The wagon body yaw is shown to stabilise quicker under the influence of the larger brake torque (Figure 5).

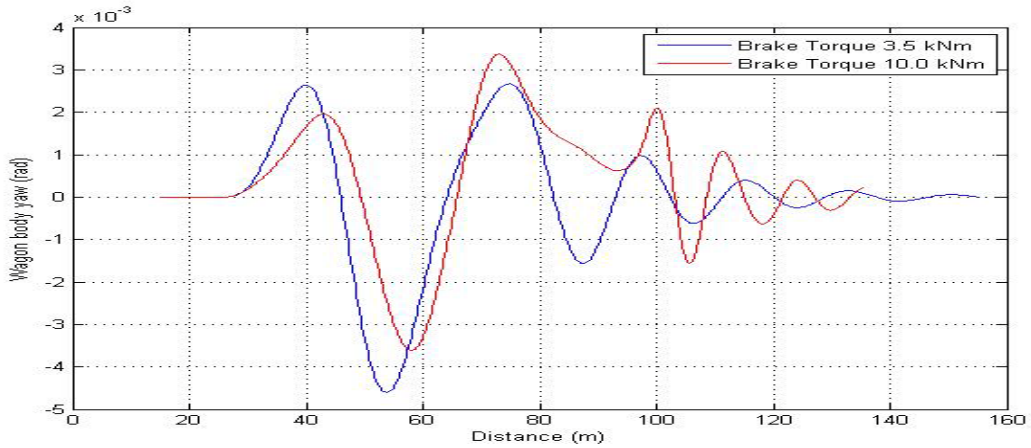

Figure 5. Wagon body yaw under brake torque

The wheel loading ratio for no torque, 3.5kNm torque and 10kNm torque cases are shown in Figure 6 that illustrates the larger wheel unloading due to larger brake torques. With the application of 3.5kNm brake torque, the wheel unloading ratio remained slightly lower than that of the no-torque case. Even for larger brake torque applications, wheel unloading ratio was still not obvious at the early stages of application; however, as the wagon moved forward the unloading ratio increased. When wheelset 4 has moved back onto the perfect rail at 85th m, only pure brake torques are involved and we can see the wheel unloading ratio further increased; however, when the brake torque is released at the 95th m, the wheel unloading ratio has quickly peaked prior to gradual damping in the natural way.

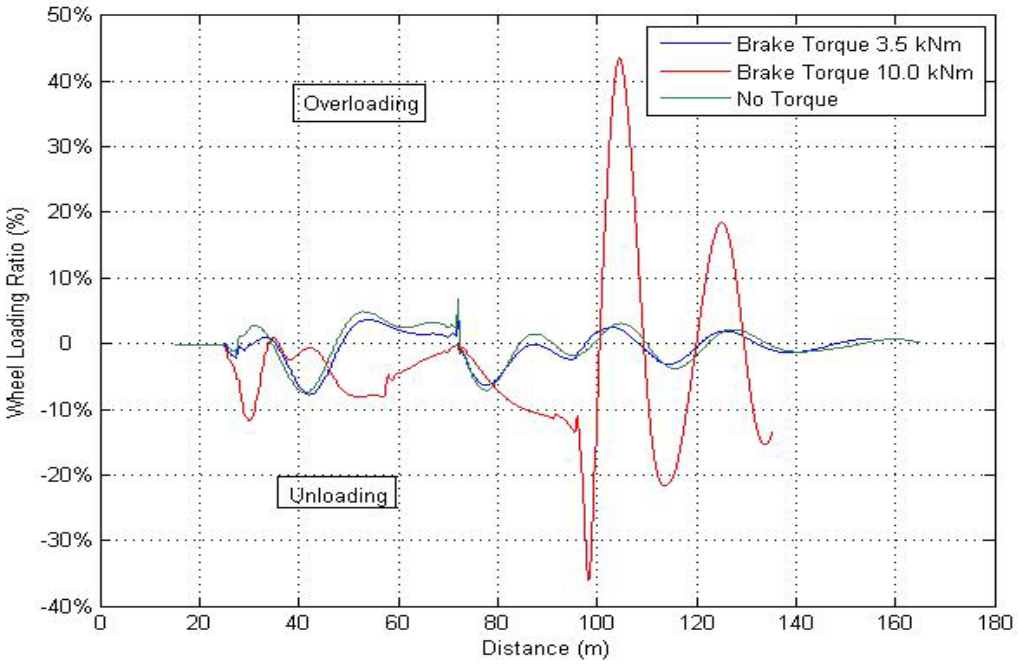

Figure 6. Wheel loading ratio (vertical) for no-torque, 3.50kNm torque and 10.0kNm torque cases

5. Effects of Track Defect on Wagon Roll

Two key signatures in isolated vertical track geometry defect variations, plateau and sinusoid, were examined. The pitch and roll of wagon body and bogies frames are presented to illustrate the effects of traction/ braking torques. All cases are simulated using 25m/s wagon speed. To this end, instantaneous and constant normal brake torque -3.5kNm, large brake torque -10kNm, normal traction torque 3.5kNm, large traction torque 10kNm, were applied.

These torques were instantaneously applied when the leading wheelset of the front bogie entered the irregularities and were held constant until the trailing wheelset of rear bogie left the irregularities, at which time the torques were instantaneously removed. Although the initail speed was set as 25m/s, these torques affected the wagon speed in a complex manner, leading to final speed in the range of 19.6m/s to 29.3m/s for sinusoid cases and 7.8m/s (for large brake case the wagon only ran 125 m rather than full 130m as the program was set to run only 8 seconds for consistency) to 34.9m/s for plateau cases. It is recognised that sudden application of such torques may not be practicable due to slackness in brake systems; as the paper is not concerned with the simulation of full braking system, just the torques were applied onto the wheelsets to demonstrate the ability of the model to handle application of braking/ traction torques.

In the simulation for vertical track irregularity (Equation(2)), k_{ir} was set at $7\times10^{-3}\,\mathrm{m}^{-1}$ and Δ_{ir} was studied as 5mm initially; in some cases the results of the 10mm defect size were also presented to show some specific features.

Three sinusoidal and one plateau defects (Figure 7) were considered in the simulation. These four cases are termed as “Case#S1”/ “Case#S2”/ “Case#S3”/ “Case#C” respectively. It can be noted that the plateau defect is longer (210m) than the sinusoid defects (160m). Thus the duration of simulation has been carried out to sinusoid and cross level defects for 6s and 8s respectively.

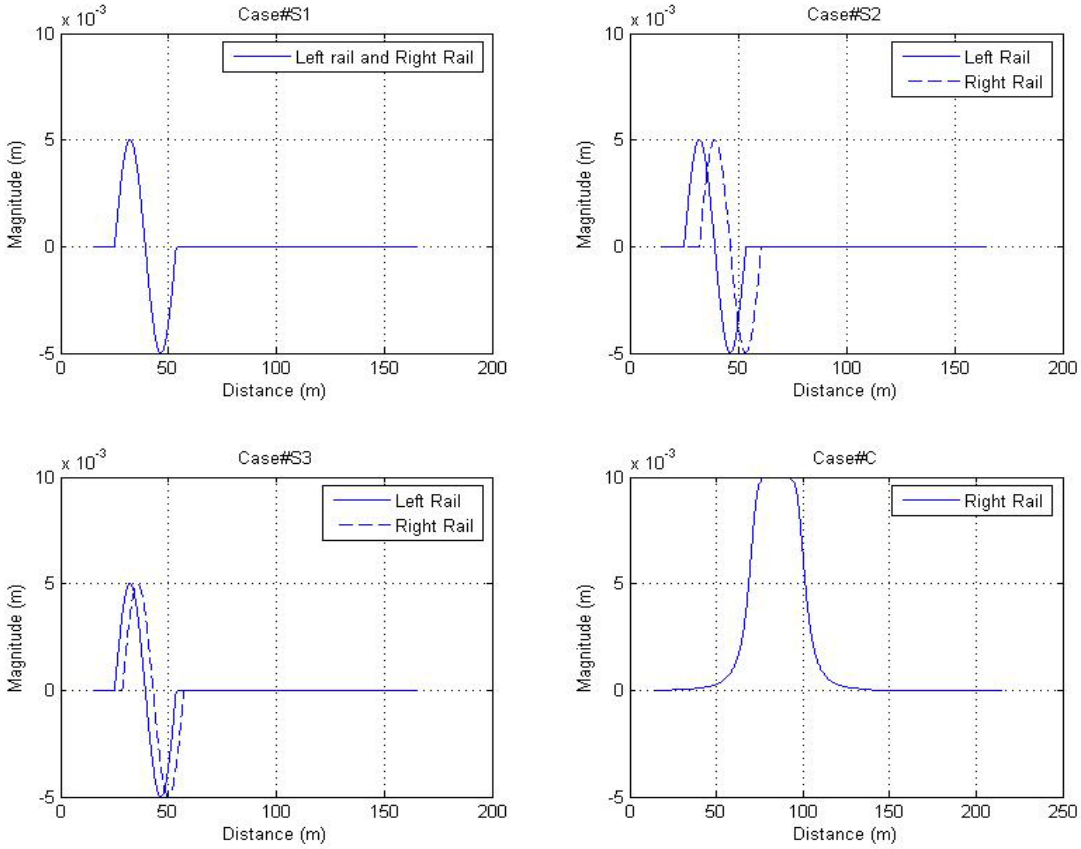

Figure 7. Sinusoid and plateau type track geometry defects

Maximum roll angles and the corresponding distances of occurrence of the front bogie/ rear bogie/ wagon body for the three sinusoidal cases are shown in Tables 2 and 3 for 5mm and 10mm defects respectively. Case#S1 provided insignificant roll irrespective of the defect magnitude.. For Case#S2 and Case#S3 scenarios, the wagon body roll angles almost doubled for the 10mm defect compared to the 5 mm defect. We can also see that Case#S2 results in the largest wagon body roll and bogie roll, the values are almost double those of Case#S3. This could perhaps be due to the rail defects of Case#S2 are offset with a larger distance compared to Case#S3 as in Figure 6. Without any torques involved, both the Case#S2 and Case#S3 show that the front bogie roll reach a peak first, followed by the wagon body roll and then rear bogie roll peaked last. This timing delay is further explored in Figure 8. We can see that the first negative and first positive peaks of wagon body roll are all located between the corresponding front and rear bogie roll peaks. However, after the wagon leaves the imperfect track, the bogies stabilised quickly while the wagon body damped in the natural

manner. A more detailed wagon modelling would have provided a faster damping characteristic. Due to Case#S1 having little effect on wagon roll, it is not further studied in Figure 8.

Table 2. Wagon body/front bogie/rear bogie positive roll and the corresponding track distance under irregularity of 5mm.

	Front Bogie ($\times 10^{-3}$ rad)	Dist (m)	Rear Bogie ($\times 10^{-3}$ rad)	Dist (m)	Wagon Body ($\times 10^{-3}$ rad)	Dist (m)
Case#S1	N/A	N/A	N/A	N/A	N/A	N/A
Case#S2	10.5	44.4	10.9	56.6	7.1	53.5
Case#S3	5.7	42.6	5.9	54.7	3.8	51.7

Table 3. Wagon body/front bogie/rear bogie positive roll and the corresponding track distance under irregularity of 10 mm.

	Front Bogie ($\times 10^{-3}$ rad)	Dist (m)	Rear Bogie ($\times 10^{-3}$ rad)	Dist (m)	Wagon Body ($\times 10^{-3}$ rad)	Dist (m)
Case#S1	N/A	N/A	N/A	N/A	N/A	N/A
Case#S2	22.0	44.5	21.1	56.6	14.2	53.7
Case#S3	11.4	42.6	11.8	54.7	7.5	51.9

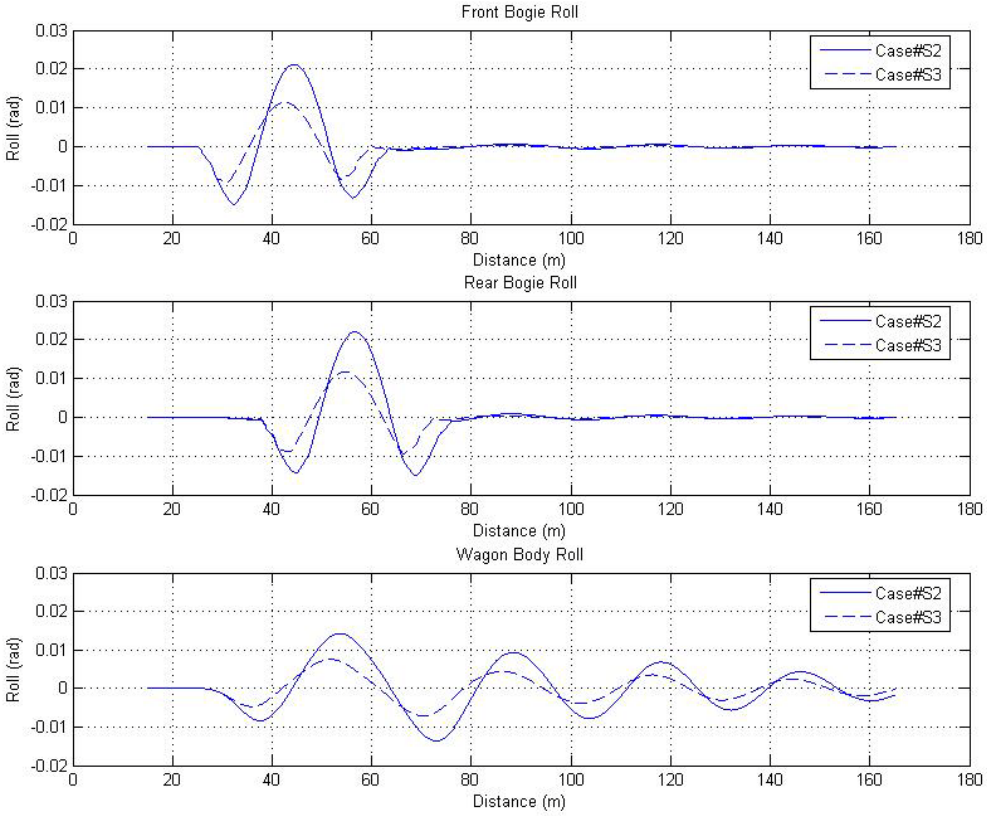

Figure 8. Front bogie/rear bogie/wagon body roll for Cases#S2 & #S3 for10mm defect

Table 4 presents the effects of the brake and traction torques applied during wheelset passage over the 5mm irregularities (S2 type). In this table, *NB* stands for normal brake torque (-3.50kNm), *LB* stands for large brake torque (-10.0kNm), *NT* stands for normal traction torque (3.5kNm), and *LT* stands for large traction torque (10.0kNm).

Since the large brake and traction torques reduce the wagon body roll to negative values from the beginning, it is meaningless to compare the initial position with the largest bogie roll location. The bogie and wagon body roll are graphically shown in Figures 9 and 10 respectively. The torque generally has only limited effects on bogie roll. The large brake torques generally increased the bogie roll while the traction effects induced far more complex behaviour of bogies and wagon.

Table 4. Torque influence on wagon system roll, Case#S2 with 5 mm irregularity

Case	Front Bogie ($\times 10^{-3}$ rad)	Dist (m)	Rear Bogie ($\times 10^{-3}$ rad)	Dist (m)	Wagon Body ($\times 10^{-3}$ rad)	Dist (m)
NoTorque-S2	10.5	44.4	10.9	56.6	7.1	53.5
NB-S2	10.9	44.3	10.9	56.6	5.6	51.7
LB-S2	12.4	44.6	12.2	57.0	N/A	N/A
NT-S2	10.2	44.2	11.1	56.6	8.6	55.1
LT-S2	11.0	44.3	11.0	57.0	N/A	N/A

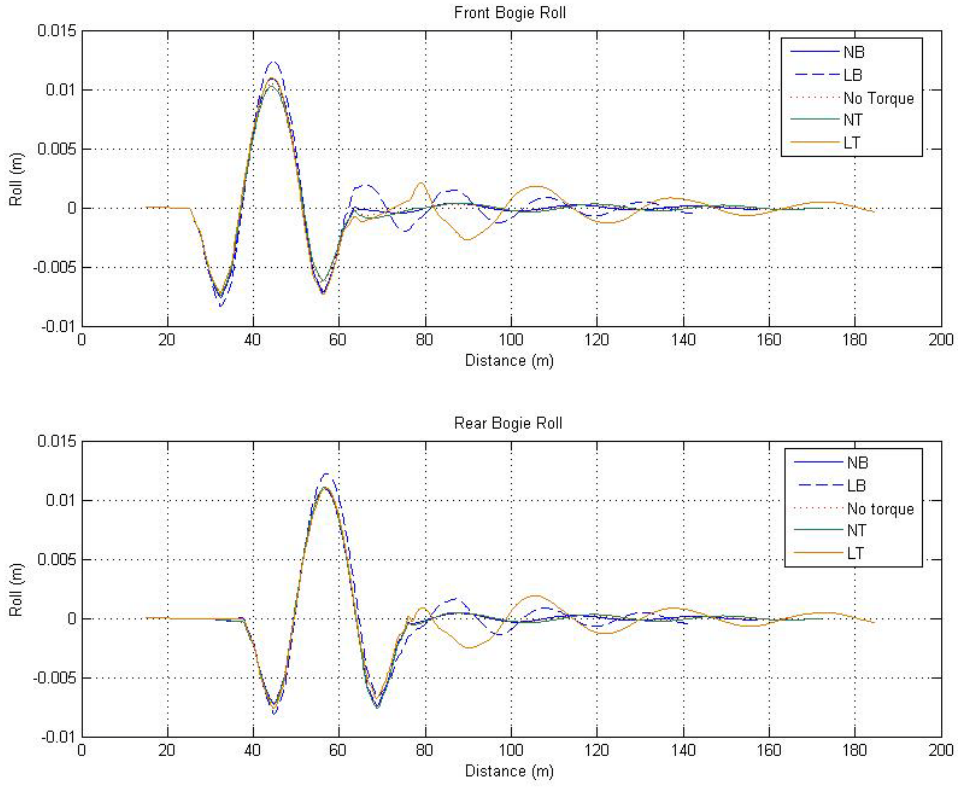

Figure 9. Front bogie and rear bogie roll for Case#S2 with 5mm irregularity

Figure 10 shows large wagon body roll (as high as 0.14 radians) under large traction (LT) and large brake (LB) applications. One of the reasons for the large roll might be the rather simplified wagon body model [1] that ignored some important components that connect the

wagon body with the frames of the bogies. For example, in freight trains, wagon body is connected with the three-piece bogie through a flat centre bowl that is secured by a pin pivot. This plate provides stiffness on all directions if contact occurs once gap clearance is closed due to longitudinal translation or roll of components. The centre plate is attached to a sturdy longitudinal beam that connects both bolsters. This beam is expected to prevent large roll of bogie components. Gap elements will be required to accurately model these components and the wagon model in [1] ignores these components and represent the connection between the wagon body and bogie frames through a series of springs and dashpots only. Further, for ease of demonstrating wagon body roll to the effects of brake/ traction torques, the wagon body was considered only partly loaded (approximately 30t); a fully loaded wagon (120t) would not have experienced such high roll. In spite of these limitations of the wagon model, the interesting feature is that even without the constraints of centre bowl and the longitudinal beam, the numerical simulation could provide results due to the wagon body maintaining varying equilibrium positions due to existence of continuous flange contact.

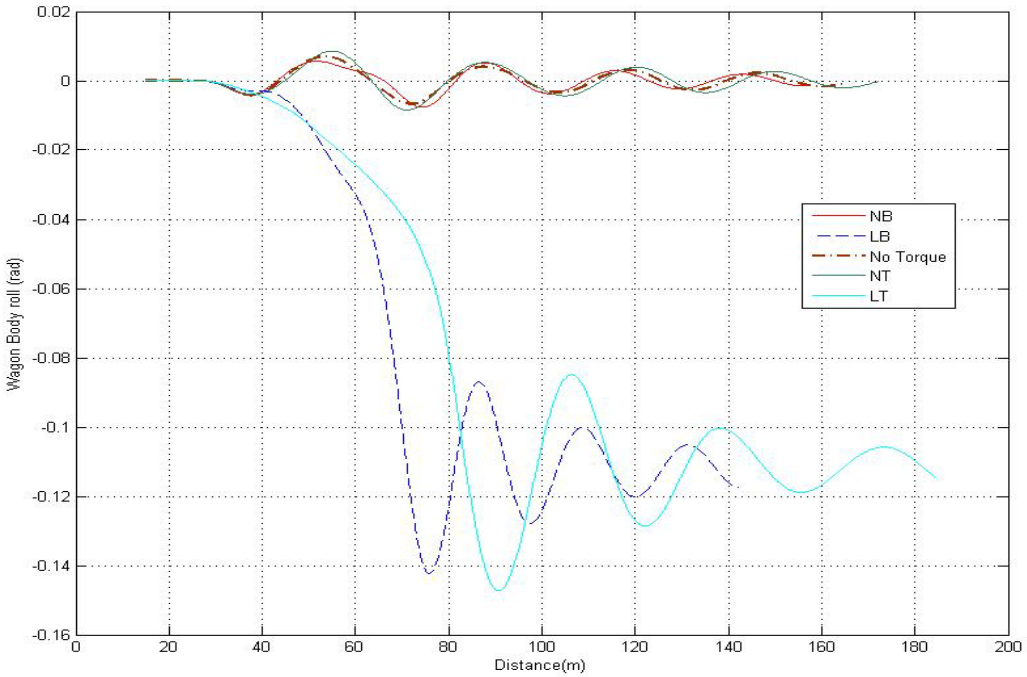

Figure 10. Wagon body roll for Case#S2 with 5mm irregularity

Case studies with irregularity magnitude of 10mm have been carried out and the bogie and wagon body roll are summarised in Table 5 and their responses are graphically shown in

Figure 11 and Figure 12 respectively. Wagon roll for the no-torque cases, exhibited linear relationship with the irregularity magnitude (for example, with the defect magnitude doubling, the roll angle doubled). When brake/traction torques are applied, this simple linear rule was no longer valid as shown in Table 6. Little difference on the front bogie and rear bogie roll (see Figure 11) can be seen among the normal brake, normal traction and no-torque cases, but the larger brake/traction torques did make the bogie roll smaller in both positive and negative values. Moreover, the large brake/traction torques have also produced the smallest roll values which occur in advance along the track compared with the other three cases. However, for no torque, normal brake and traction torque cases, the wagon/bogie roll are still roughly doubled from 5mm case to 10mm cases.

Table 5 Torque influence on wagon system roll, Case#S2 with 10mm irregularity

Cases	Front Bogie ($\times 10^{-3}$ rad)	Dist (m)	Rear Bogie ($\times 10^{-3}$ rad)	Dist (m)	Wagon Body ($\times 10^{-3}$ rad)	Dist (m)
S2	22.0	44.5	21.1	56.6	14.2	53.7
NB-S2	22.5	44.4	22.2	56.6	11.7	51.5
LB-S2	13.2	42.8	12.8	55.2	N/A	N/A
NT-S2	20.9	44.4	22.5	56.8	18.3	55.9
LT-S2	11.8	42.6	11.5	55.2	N/A	N/A

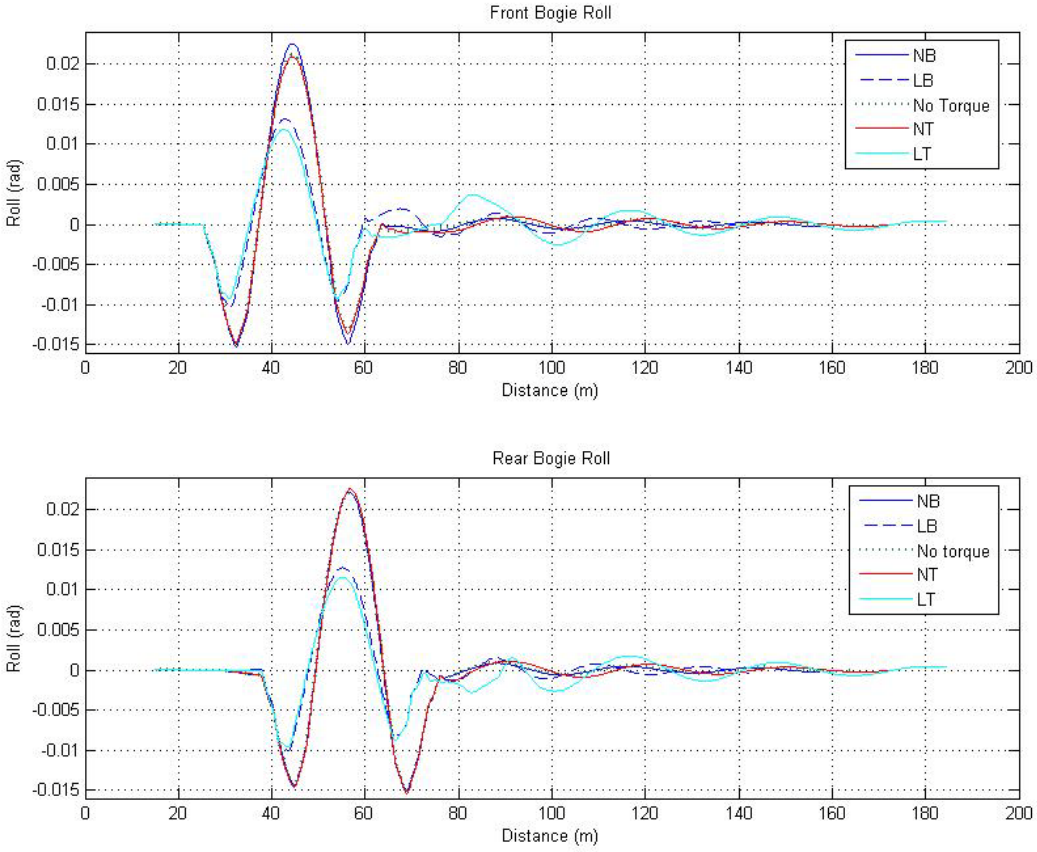

Figure 11. Front bogie and rear bogie roll for Case#S2 with 10 mm defect

In Figure 12, the LB and LT torques increased the wagon body roll and restricted its movement between -0.09 rad to -0.15 rad; this level being much higher in absolute terms than that of the other three cases. This can be explained through Figure 13 that shows the wagon lateral displacements. It is interesting to see that the LB and LT torques held the wagon body to one side after both bogies peaked and the torques were released; the wagon body then damped but maintained a higher level of lateral displacement than the balance position.

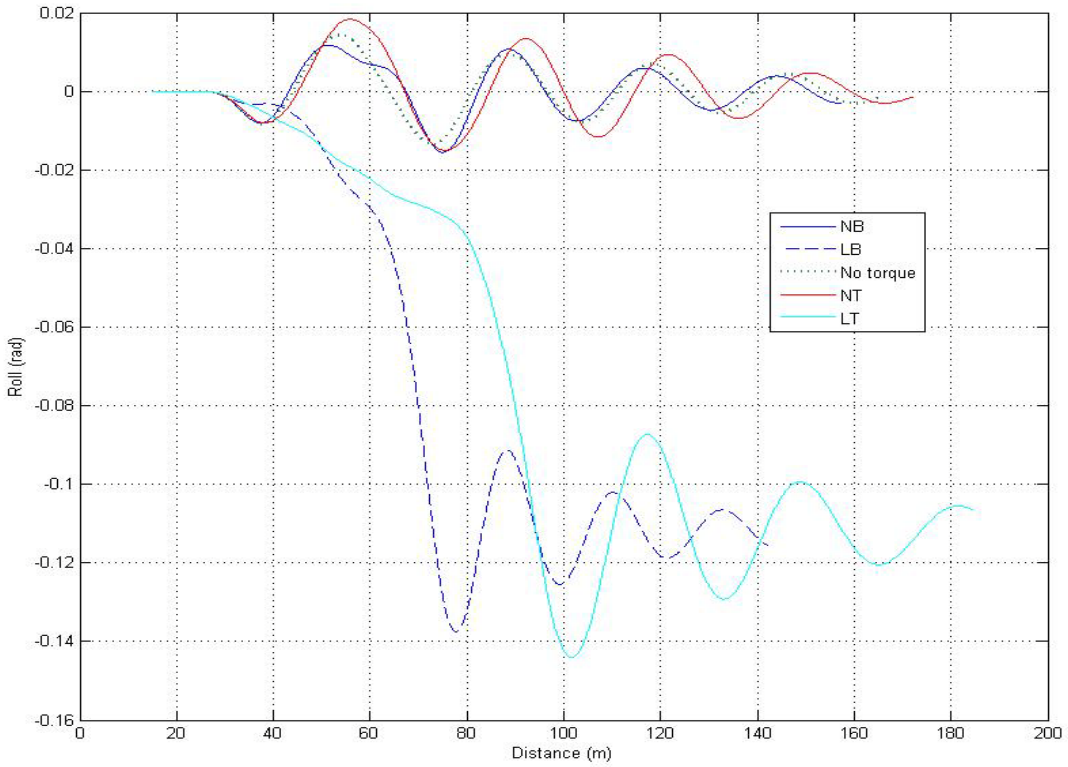

Figure 12. Wagon body roll for Case#S2, with 10mm irregularity

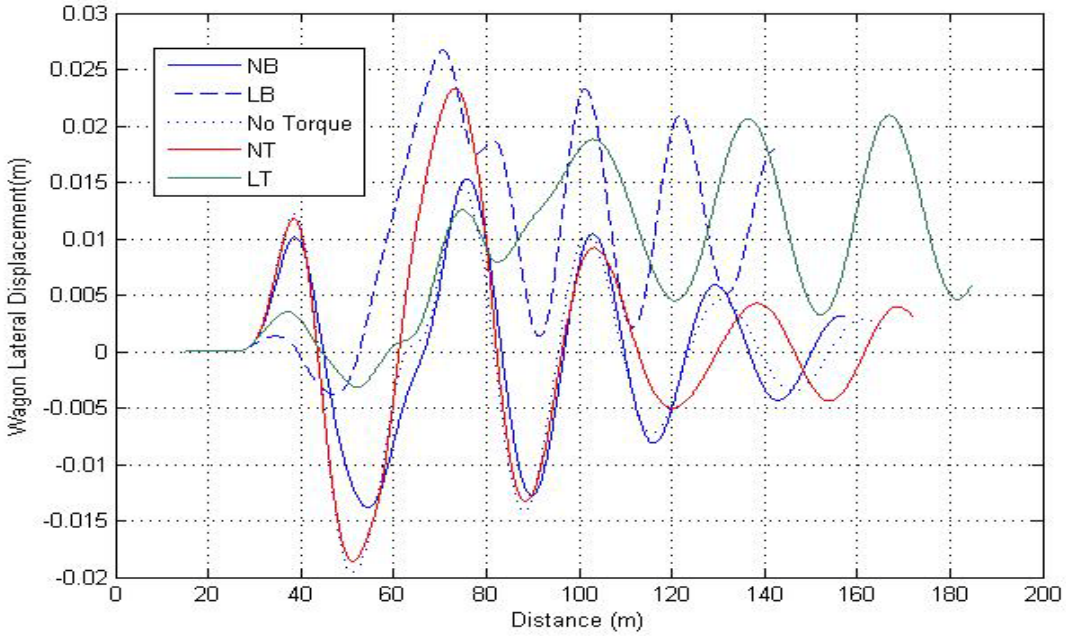

Figure 13. Wagon body lateral displacements for Case#S2, with 10mm irregularity

Under cross level (see Figure 14), the large brake torque sustained considerably negative wagon body roll while the large traction torque did not produce this effect; however, from the 100th m until the 160th m, the large traction torque did keep the wagon body roll negative, until after the brake torque was released at the 155th m of travel. The NB and NT torque cases did not cause any alarming body roll as the LB case. In both LB and LT Cases#S2 as shown in Figure 11, the wagon body roll increased with the existence of torque, and after torques were released at 76m, they both failed to return to its original balanced positions. However, the cross level shows a different pattern: after torque was released, the LT returned to the balanced position with the speed around 34.9m/s(125.6km/h) while such a recovery did not occur with the LB case.

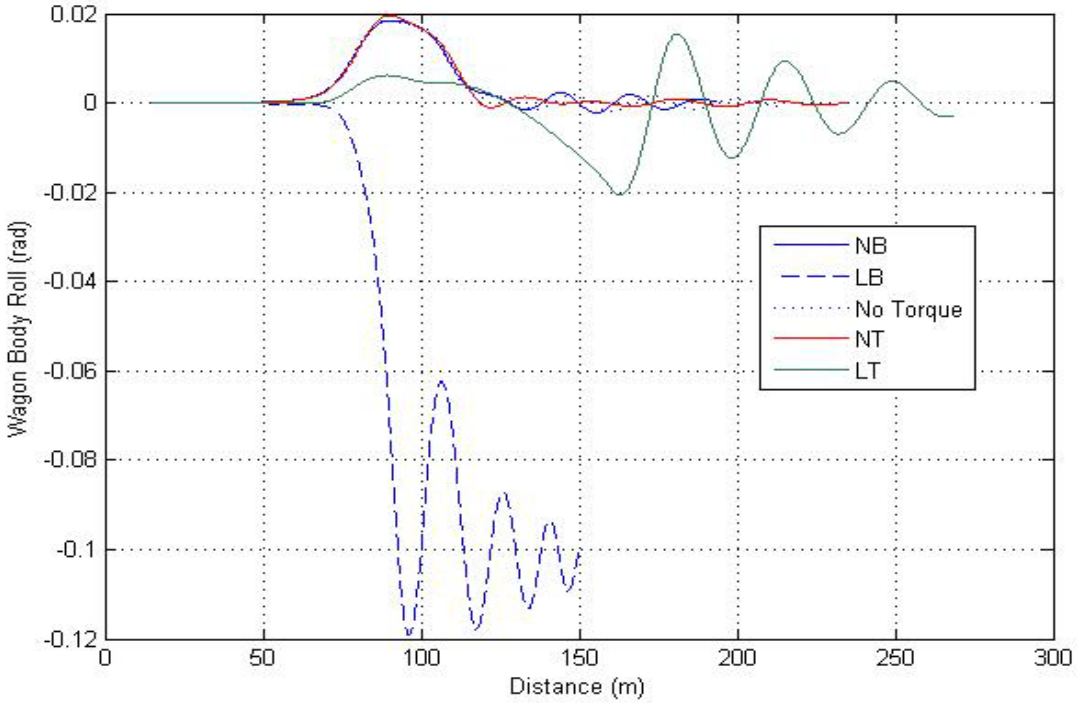

Figure 14. Wagon body roll for Case# C

The phenomenon of large wagon body roll under LT and LB torques shown in Figures 12 and 14 could be explained using the simplified modelling in [1] as was done for Figure 10. The large roll of the wagon body occurred after the roll of both bogies peaked with the wagon body failed to return to the initial position, but maintaining a new equilibrium position by maintaining the flange contact even after the torques were released. In real wagons, after

peaking of both bogie rolls, the centre bowl and the longitudinal beam would have restored the wagon to its initial equilibrium position rather than sustaining flange contact.

6. Effects of Track Defect on Wagon Pitch

This section reports the wagon pitch. Initially a series of smaller magnitude vertical track irregularities are presented to reveal the distinguishing features, then the larger magnitude irregularities are reported (see Table 6 and Table 7).

Table 6. Bogie and wagon pitch for Case#S1, #S2 & #S3 with 5mm irregularity

Cases	Front Bogie (10^{-3} rad)	Dist (m)	Rear Bogie (10^{-3} rad)	Dist (m)	Wagon Body (10^{-3} rad)	Dist (m)
Case#S1	2.2	40.6	2.2	53.1	2.6	48.9
Case#S2	1.5	44.1	1.5	56.5	1.8	52.5
Case#S3	2.0	42.4	2.0	54.9	2.4	50.6

Table 7. Bogie and wagon pitch for Case#S1, #S2 & #S3 with 10mm irregularity

	Front Bogie (10^{-3} rad)	Dist (m)	Rear Bogie (10^{-3} rad)	Dist (m)	Wagon Body (10^{-3} rad)	Dist (m)
Case#S1	4.4	40.6	4.4	53.1	5.2	48.7
Case#S2	3.1	44.0	3.1	56.3	4.0	52.9
Case#S3	4.0	42.4	4.0	54.9	5.0	50.7

Similar to the wagon roll, where no-torque is applied, the larger irregularity magnitude would cause larger wagon pitch, and the corresponding wagon body pitch always occurs between the front bogie and rear bogie. The longitudinal track differences also convey corresponding wagon body/front bogie/rear bogie pitch delay.

Torque influence on wagon system pitch is presented in Table 8.

Table 8. Torque influence on wagon system pitch, Case#S2, 5mm irregularity

Cases	Front Bogie ($\times 10^{-3}$ rad)	Dist (m)	Rear Bogie ($\times 10^{-3}$ rad)	Dist (m)	Wagon Body ($\times 10^{-3}$ rad)	Dist (m)
No Torque - S2	1.5	44.1	1.5	56.5	1.8	52.5
NB-S2	1.6	44.1	1.6	56.6	2.0	52.5
LB-S2	1.9	44.0	1.9	56.8	1.6	53.4
NT-S2	1.4	44.1	1.5	56.5	1.8	53.3
LT-S2	1.2	44.2	1.2	56.4	2.4	51.5

The maximum front bogie pitch and rear bogie pitch occur almost at the same longitudinal distance (44.1 m for the front bogie; 56.5m for the rear bogie), indicating the predominance of the track geometry profile onto the dynamic response signature. The peak values of front bogie pitch and rear bogie pitch under brake torque are larger than the no-torque cases; traction torques have the capability to reduce the wagon pitch and bogie pitches below the no-torque cases. These characteristics were similar to the published graphics in [1]; therefore, no further graphics shown.

Table 9 illustrates that the normal brake/traction does not influence either the maximum bogie pitch (magnitude) or the corresponding track distance (location). However, similar to the wagon body roll, for combinations of large brake/traction torques and larger magnitude irregularities, the corresponding track distance of the maximum value of the bogie pitch was ahead of other three cases and their values also were higher.

Table 9. Torque influence on wagon system pitch, Case#S2, 10mm irregularity

Cases	Front Bogie ($\times 10^{-3}$ rad)	Dist (m)	Rear Bogie ($\times 10^{-3}$ rad)	Dist (m)	Wagon Body ($\times 10^{-3}$ rad)	Dist (m)
No Torque - S2	3.1	44.0	3.1	56.3	4.0	52.9
NB-S2	3.2	44.1	3.2	56.4	3.8	52.5
LB-S2	4.3	42.2	4.4	54.9	3.9	51.4
NT-S2	3.0	43.9	3.0	56.4	4.0	53.9
LT-S2	3.6	42.4	3.7	54.9	5.3	87.8

7. Studies on the Effects of Worn Rail and Wheel Profiles

The profiles of the railhead and wheel tread change during operation due to natural wear; the worn rail/wheel usually results in extra energy consumption, higher impact forces and accelerated rail/wheel wear. Of great importance to study of the worn rail/wheel, is to spline their profiles, which usually suffers from the resolution of the measured data. Technically, the flange contact could be studied but larger inaccuracy may occur since the spline wheel profile has singularity at flange. In this section, only the wheel lateral forces, wheelset slip and wagon travel distances are reported due to worn rail/ worn wheel analyses; for ease of understanding the data, either the rail or the wheel was considered worn – not both the rail and the wheel in a single analysis.

7.1 Worn Rail Study

Figure 15 exhibits the wheelset on the center of narrow gauge track (1067mm) used in Australia, with the nominal distance between the wheel and the rail of 1140mm. For the new wheel - rail contact point positions, the nominal width and height were 570mm (half of 1140mm shown in Fig. 15) and 0mm respectively; whereas, for the worn rail - new wheel

contact, the contact point would have a different width and height values, dependent on their relative worn intensities.

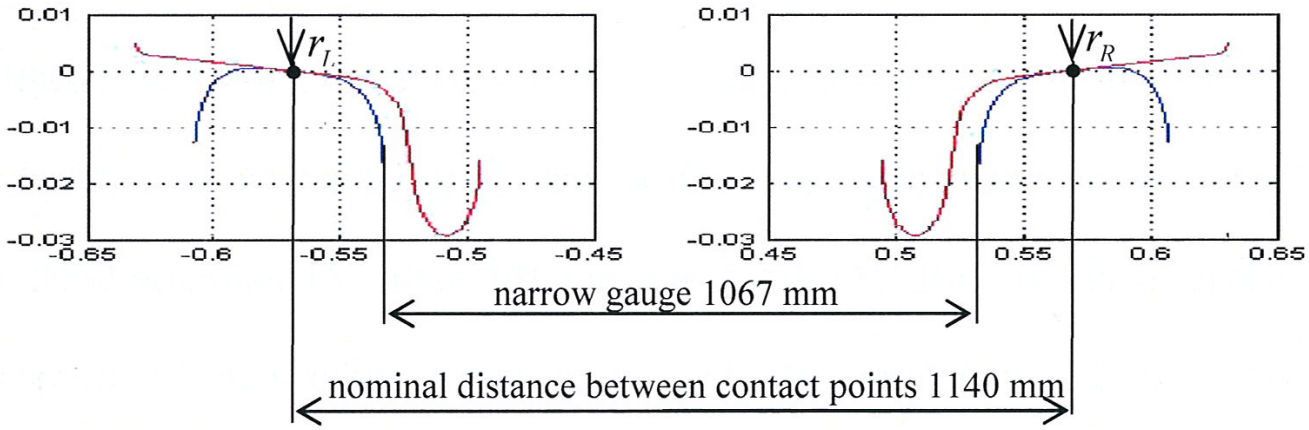

Figure 15. Wheelset on narrow gauge track

A measured worn rail is shown in Figure 16, which is typical of railhead wear (also known as table wear). Rails are normally fitted with a cant of 1 in 20 inclination. With the help of Spline2 V6.0 software [22], the worn rail profile spline representation was generated using a fifth order polynomial. Derivatives of the rail profile are fitted with relatively smooth curves that are continuous up to the third derivatives.

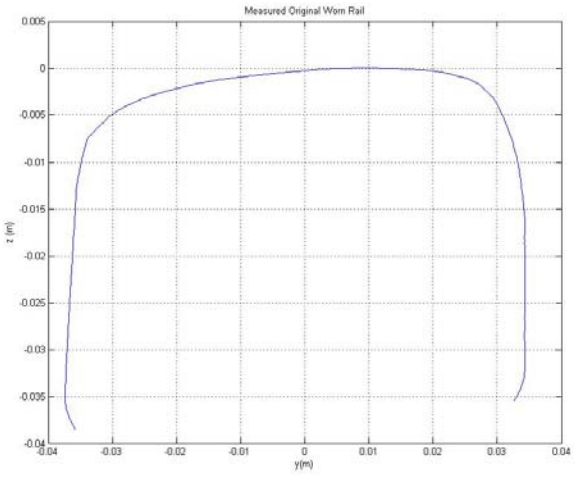

Figure 16. Measured worn rail

In order to examine the effect of the worn rail to brake torques, two sets of brake torques, Sequenece#1 and Sequence#2 as shown in Figure 17, were applied on each wheelset from t=1 second to t=5 seconds. The initial speed of the wagon was set as 25m/s as used in previous case studies. Given the new wheel radius 0.425m, the initial wheelsets angular velocity would be 58.8 rad/s.

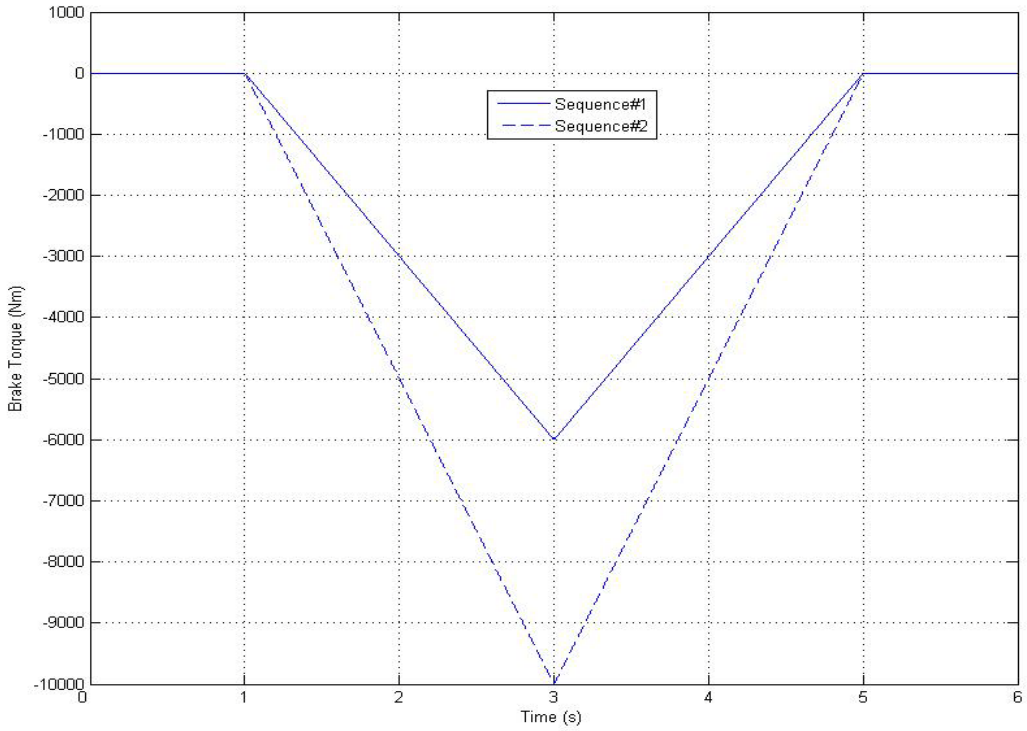

Figure 17. Input brake torque

The new rail/new wheel case studies are termed as Case#nr1 and Case#nr2 respectively for the application of Sequenece#1 and Sequence#2 brake torques (Fig. 17). The worn rail/new wheel case studies are termed as Case#wr1 and Case#wr2 respectively for the application of Sequenece#1 and Sequence#2 brake torques.

Figure 18(a) shows wheel lateral forces under gentle brake torque (Sequence #1) application for both the new and the worn rails. The wheel lateral force decreases with the increase in brake torque (refer to Figure 18(a) and Figure 17, sequence#1) and reaches its peak value at the 3rd second where the brake torque was maximum. Then the wheel lateral force increased to the original value after brake torque was released. Beyond the brake application time t=1

second to t=5 seconds, the wheel lateral force remained steady. For the larger brake torque application sequence#2 (see Figure 17), Figure 18 (b) shows a distinct feature. After the wheel lateral forces achieved their peak at t=3seconds, it did not remain steady as in Figure 18(a) for Sequence#1, even though the brake torque was released at t=5seconds; however, no flange contact was observed, which re-confirmed that the changes to the lateral force (Figure 18) was solely due to the effects of brake torque (Fig. 17). This can be seen from the lateral force diagram for the left wheel of the same wheelset plotted in Figure 19; only Sequence#2 is shown. From Figure 18(b) and Figure 19, equilibrium in the lateral direction can be observed – without any need for flange contact.

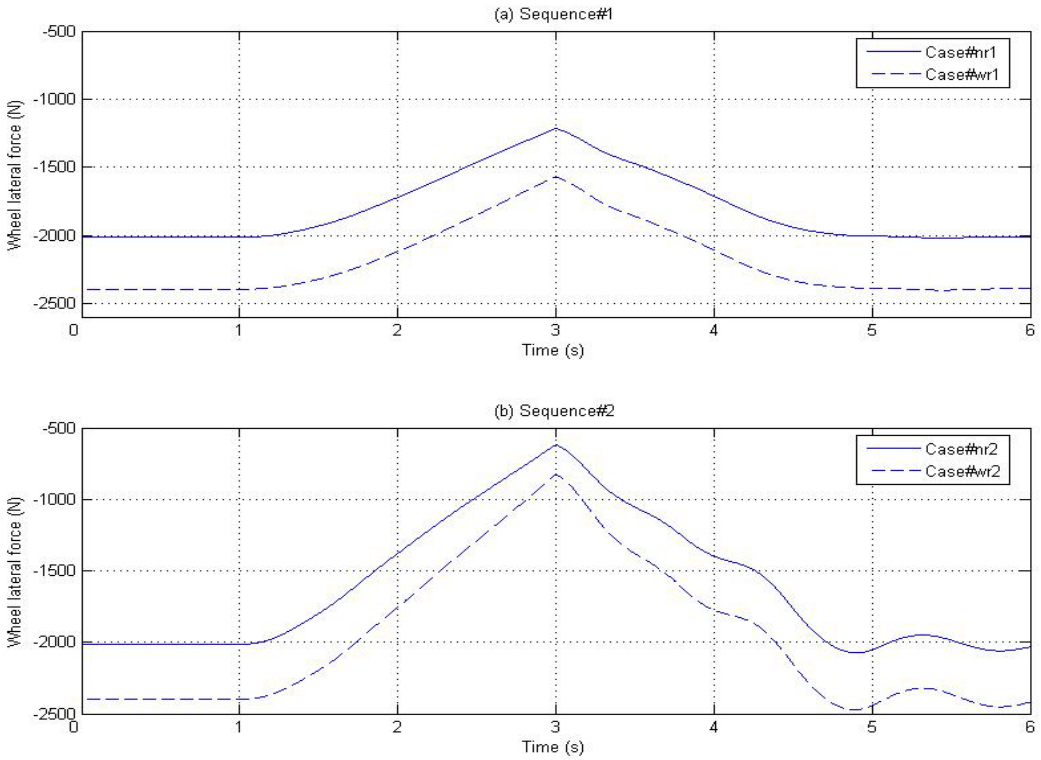

Figure 18. Lateral forces of right wheel of the first wheelset:rail cases

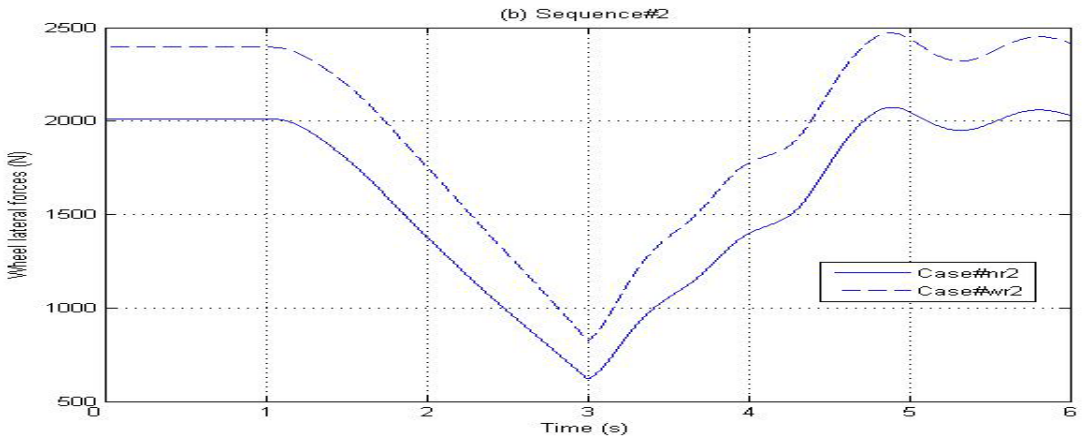

Figure 19. Lateral forces of left wheel of the first wheelset: rail cases, Sequence#2

The difference between the angular velocity of the wheel and the corresponding longitudinal velocity leads to wheel slip. In [19], the slip rate calculated was about 5%, but the brake torque applied to the wheelset was constant (5,000 Nm) and the total mass was much smaller. The manner in which the brake torques were applied (Figure 17) in this paper is more complex than the treatment in [19]: however an approximate calculation can confirm that the slip rate for the cases considered in this paper is similar that published in [19]. For example, the initial speed of 25.0m/s at t=1second at the commencement of brake torque has reduced to 22.3032m/s at t=5second when the brake torque was released; this represents an average deceleration over the four seconds of brake application of 0.6742m/s^2 (which includes slip). By considering the average torque of 3000Nm (for cases #nr1 and #wr1, see Figure 17), the total torque on the wagon system applied to the four wheelsets would be 12,000Nm. Using the mass of the wagon (wagon body (30t) + two bogie frames (2 × 2.5t) + four wheelsets (4 × 1.12t)) as 39,480kg and the radius of the wheels as 0.425m, the deceleration can be worked out as (12,000/(39480×0.425)) = 0.7152m/s^2, which shows the computer model predicted deceleration (0.6742m/s^2) is approximately 5.7% smaller. Therefore, it can be claimed that the slip under the brake torque sequence#1 (Figure 17) is approximately 5.7%. Further results from the analyses are shown numerically in Table 10, which lists the actual wheelset rotation angle, the actual travel distance, and the no slip travel distance, for new rail and worn rail cases. The actual travel distance (m) and the wheelset rotation angle (radians) were obtained from the results of the analysis program. The no-slip travel distance was calculated by multiplying the wheelset rotation angle with the wheel radius (0.425m). The results show that the worn rail marginally increase the slip and the increase in slip is more pronounced for

severe brake application. Note the reported distance is the total distance travelled that includes 2 seconds of no torque and 4 seconds brake torque travel time.

.Table 10. Travel distances for the new rail and worn rail

Case	Wheelset rotation angle (rad)	No-slip travel distance (m)	Actual travel distance (m)	Slip (mm)	Effect of worn rail (mm)
Case#nr1	333.6857	141.8164	141.8556	39.2	+0.255%
Case#wr1	333.6807	141.8143	141.8536	39.3	
Case#nr2	320.8581	136.3647	136.4413	76.6	+0.261%
Case#wr2	320.8531	136.3626	136.4394	76.8	

Figure 20 shows the wheelset angular velocity difference for new rails. As identified in Table 10 and Figure 18, this rail profile is only marginally worn and hence the slip rate is not much different between the new and worn rail cases. It can be seen that the slip occurs in a fraction of second and it increases with the increasing braking torque. For Case#wr1, it shows approximately linear proportional increases with a maximum value 0.0476. For Case#wr2, it shows nonlinear characteristics with a maximum value 0.1072.

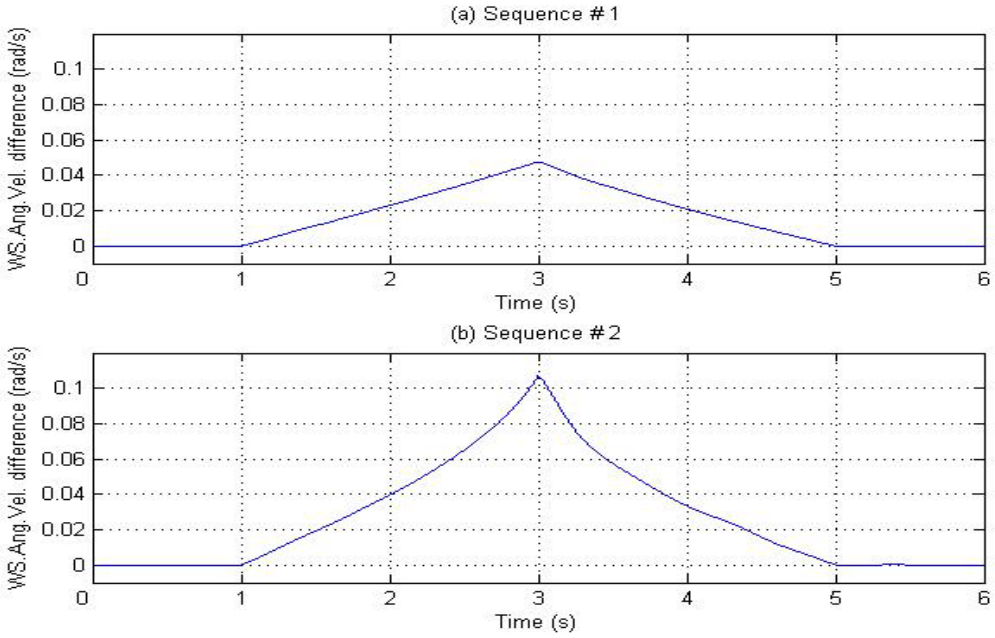

Figure 20. Angular velocity difference of wheelset under normal and severe brake torques

7.2 Worn Wheel Study

A measured original worn wheel is shown in Figure 21. Unlike the rail profile, derivatives of the wheel profile were not so smooth especially at the flange area; therefore only the smooth wheel tread part data wereused in the simulation. Unlike the worn rail (Figure 16), the wheel considered (Figure 21) is seriously worn and is defined as 'hollow-worn' with 2.9mm wear.

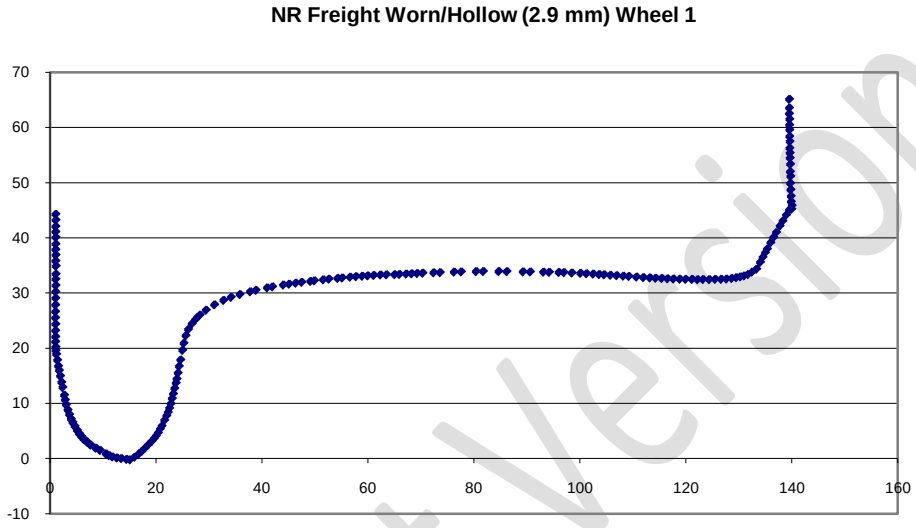

Figure 21. The measured profile of the worn wheel used (Y axis dimensions shown horizontally and Z axis dimensions shown vertically. All units: mm)

The new wheel/new rail, case studies Case#nw1 and Case#nw2 correspond to Sequenece#1 and Sequence#2 respectively are already discussed in Table 10; the worn wheel/new rail, case studies Case#ww1 and Case#ww2 correspond to Sequenece#1 and Sequence#2 respectively are new and specific to this Section 7.2.

Figure 22 exhibits the lateral forces of right wheel of the first wheelset. In Figure 22 (a), during the brake torque application from t=1 to t=3 seconds, both the new wheel and the worn wheel generally have shown linear reduction; however, after brake torque is released at 5^{th} second, worn wheel has shown non-steady state while the new wheel has remained steady. Turning attention to Figure 22 (b), even at the first 2 seconds of brake application, the worn wheel exhibits non-linear characteristic, after t=5 seconds, the situation has remained similar to the Case#ww1. The forces jumped at the end of 6^{th} second in Case#ww1 and the flange contact force was expected to push the wheel back to conventional position. However, as

stated previously, the flange area of wheel was not modelled, so there was no flange contact force to push the wagon back to equilibrium position. The computer program failed to converge shortly because no contact points (in flange area) could be found. The reduction in the lateral force, due to no-flange contact, is solely attributed to the characteristics of teh applied brake torque.

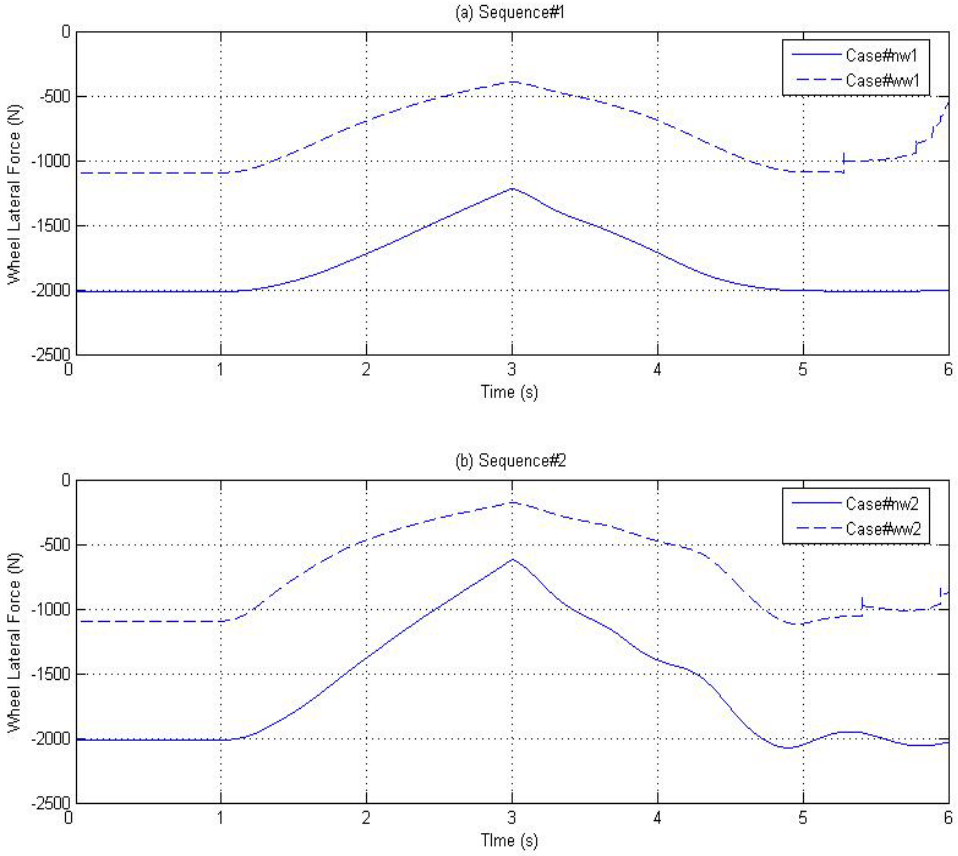

Figure 22. Lateral forces of right Wheel of the first wheelset—wheel cases

The travel distance is summarised in Table 11. The worn wheels have shown worse performance on wheel lateral forces; however, the corresponding travel distance was the shortest amongst the cases studied. This phenomenon confirms the operational matters where the drivers report better vehicle stability with hollow worn wheels. The severely worn wheel considered in this section has exhibited pronounced effect (-16.58% and -16.71%) of reduction in slip compared to their respective new wheel cases (Table 11).

Table 11. Travel distances for the new wheel and worn wheel

Case	Wheelset rotation angle (Rad)	No slip travel distance (m)	Actual travel Distance (m)	Slip (mm)	Effect of Worn Wheel (%)
Case#nw1**	333.6857	141.8164	141.8556	39.2	-16.58%
Case#ww1	333.6952	141.8205	141.8532	32.7	
Case#nw2**	320.8581	136.3647	136.4413	76.6	-16.71%
Case#ww2	320.8823	136.3750	136.4388	63.8	

** these results are as same as Case#nr1, Case#nr2 since the rail and wheel profile are same.

8. Conclusions

A fixed coordinate system formulation for the rigid multi-body rail wagon dynamics presented earlier by the authors is reviewed. The formulation employs a three-dimensional contact model with full parameterisation of the surfaces of the two contacting bodies. The benefit of the formulation is its ability to determine roll of the wagon components, which other standard commercial packages cannot determine. Further the model does not require setting up of speed profile as *a priori* since the speed is determined as a result of the applied brake/ traction torque.

Several numerical examples were studied to examine the effects of brake/ traction torque on tracks with various types and levels of irregularities. The following conclusions were made:

- The wagon yaw, pitch and roll exhibit a positive propositional relationship to the track defect amplitude.
- Large brake (LB) torque results in large wheel unloading ratio to the track lateral irregularity; wagons under normal level of braking or no-torque (steady state case) do not suffer wheel unloading due to track irregularities considered in this paper. =
- With the increase in the longitudinal phase difference of the sinusoid irregularity between the left/right rails (cross level), the wagon roll increases. Cross level defects also determines when the largest wagon body/bogie roll is likely to occur.

- The sinusoidal track irregularity effect on wagon roll is more severe than the cross level irregularity induced wagon roll in the model consider in this paper.
- The normal torques generally do not induce bogie roll; however, large external torques can affect the wagon body roll.
- Large brake torque generally increases the absolute value of the wagon body roll whilst the traction effects induce far more complex dynamics of bogies and wagon body.
- If no brake torque is applied on the worn wheel/rail, steady wheel lateral forces can still be achieved.

References

1. Z. Zhang, and M. Dhanasekar, Dynamics of railway wagons subjected to braking/traction torque, Vehicle Syst. Dyn. 47 (3) (2009), pp. 285 – 307.
2. M. Mcclanachan, C.Cole, D.Roach, AND B.Scown, An Investigation of the Effect of Bogie and Wagon Pitch Associated with Longitudinal Train Dynamics, The Dynamics of Vehicles on Roads and on Tracks, Vehicle Syst. Dyn. Suppl.(33) (1999), pp. 374-385.
3. D. Climb, J. Wagner, AND A.Baviskar, Investigation of active torsion bar actuator configurations to reduce vehicle body roll. Vehicle Syst. Dyn. 44 (9), (2006) pp.719-736.
4. R. V. Dukkipati, Vehicle Dynamics, Boca Raton, Fla, CRC Press, 2000.
5. A. A. Shabana, AND J. R. Sany, A Survey of Rail Vehicle Track Simulation and Flexible Multibody Dynamics. Nonlinear Dyn. 26(2) (2001), pp.179-210.
6. J. Pombo, J. A**mbrósio**, AND M.Silva, A new wheel–rail contact model for railway dynamics, Vehicle Syst. Dyn., 45 (2) (2007), pp165-189.
7. G. X. Chen, AND X.C. Jin, A Simulation Study on Influence of Periodic Irregularities on Derailment safety of a Freight car on Tangent Track, Proceedings 7th International Heavy Haul Conference, Brisbane, Australia, 2001, P.533.
8. D. Li, A. Meddah, K. Hass, AND S. Kalay, Relating track geometry to vehicle performance using neural network approach, I Mech E Part F: J. Rail and Rapid Transit, 220 (3)(2006), pp.273-281.

9. M.J.M.M. Steenbergen, The role of the contact geometry in wheel–rail impact due to wheel flats, Vehicle. Syst. Dyn. 45(12) (2007), pp. 1097-1116.
10. M.J.M.M. Steenbergen, The role of the contact geometry in wheel-rail impact due to wheel flats: Part II, Vehicle Syst. Dyn, 46(8) (2008), pp.713 -737.
11. M. A.Murtaza, AND S.B.L. Garg, Parametric study of railway air brake system, I Mech E Part F: J. Rail and Rapid Transit, 206(1992), pp.21-36.
12. T.Piechowiak, Pneumatic train brake simulation method, Vehicle Syst. Dyn. 47(12) (2009), pp.1473-1492.
13. G. Cocci, P. Presciani, A.Rindi, AND G. P. J. Volterrani, Railway wagon model with anti slip braking system. 16th European MDI user conference. Berchtesgaden, Germany, 2001.
14. M.Chou, AND X. Xia, Optimal cruise control of heavy-haul trains equipped with electronically controlled pneumatic brake systems, Control Engineering Practice, 15 (5)(2007), pp.511-519.
15. B. J. Olson, Nonlinear Dynamics of Longitudinal Ground Vehicle Traction, Mechanical Engineering. Michigan, USA, Michigan State University, 2001.
16. M. Malvezzi, P. Presciani, B. Allotta, AND P. Toni, Probabilistic Analysis of Braking Performance in Railways, I Mech E Part F: J. Rail and Rapid Transit, 217(3) (2003), pp.149-165.
17. M. Durali, AND B. Shadmehri, Nonlinear Analysis of Train Derailment in Severe Braking, J. of Dyn. Syst., Measurement, and Control, 125(1) (2003), pp.48-53.
18. C. Cantoni, R. Cesarini, G. Mastinu, G. Rocca, R.Sicigliano, Brake comfort - a review, Vehicle Syst. Dyn. 47(8) (2009), pp.901 -947.
19. Y. Handoko, AND M. Dhanasekar, An Inertial Reference Frame Method for the Simulation of Effect of Longitudinal Force to the Dynamics of Railway Wheelsets, Nonlinear Dyn. 45(3-4) (2006), pp.399-425.
20. Y. Handoko, AND M. Dhanasekar, Wheelset Skid in Railway Bogies, I Mech E Part F: J. Rail and Rapid Transit, 221(2) (2007), pp237-245.
21. Y. Handoko, Investigation of the Dynamics of Railway Bogies Subjected to Traction /Braking Torque, Ph.D dissertation., Center for Railway Engineering. Central Queensland University, Australia, 2006.
22. B. J. Thijse, Spline 2 V6.0 Software, Delft University of Technology, Laboratory of Material Science, Delft, 2002.